Effects of obesity on time-frequency components of electroretinogram signal using continuous wavelet transform

Okan Erkaymaz [a], İrem Senyer Yapici [b],[*], Rukiye Uzun Arslan [b]

[a] *Department of Computer Engineering, Zonguldak Bülent Ecevit University, Zonguldak, Turkey*
[b] *Department of Electrical and Electronics Engineering, Zonguldak Bülent Ecevit University, Zonguldak, Turkey*

ARTICLE INFO

ABSTRACT

We investigate impacts of the obesity on three different responses (cone, rod and maximal combined) of electroretinogram signals. To analyze and extract features of the responses, two major components of electroretinogram signal (namely "a" and "b" waves) have been used. The amplitudes and respective peak times of the waves have been firstly calculated by using statistical methods in time domain. These time domain analysis could be integrated by time-frequency domain analysis to reflect electroretinogram components considerably. To achieve this aim, we have analyzed the "a" and "b" waves by applying short time Fourier transform, continuous wavelet transform and discrete wavelet transform methods on electroretinogram signals. Our findings prove that the continuous wavelet transform gives better results than other methods with respect to time-frequency results extracted from scalogram analyses. In this context, it is also showed that the usage of Mexican hat is the most proper wavelet to analyze obesity effect on electroretinogram. Moreover, we show that the "a" wave does not change considerably by obesity for electroretinogram responses. On the contrary, the "b" wave is significantly affected from obesity for maximal combined response as compared with other responses. The novelty of this work lies in the fact that the present paper is the first attempt to address the effects of obesity on electroretinogram signals. Furthermore, it is clearly denoted that the electroretinogram signals are affected adversely with levels of the obesity.

1. Introduction

The retina is the eye tissue layer including photosensitive (light-sensitive) nerve cells that provide vision [1]. These photosensitive cells have been activated by a stimulus presented to the retina. Hereby, an electrical response is obtained which enables the examination of the retina. This response that can be measured by electrodes placed on the cornea or inner surface of the retina is named as electroretinogram (ERG) [2–4].

A typical ERG signal comprises four waves called "a", "b", "c" and "d". Each of them represents the excitation response of a different layer of the retina [5,6]. Here; "a" wave is the response of the photoreceptive layer, "b" wave is the response of the bipolar-Müller cell complex, "c" wave is the response of pigment epithelium layer and "d" wave is the closure response at the end of stimulation [7–11]. In addition to these waves, in an ERG signal, it has been determined that diverse waves such as "i" wave and photopic negative response (PhNR) are also present, which have been found to occur only under special conditions related to

the data collection method [12]. Most of the studies in literature have been focused on time domain analysis of "a" and "b" waves where their effects on ERG signal are clearly known [12,13]. For example, Barraco et al. have performed time-frequency analysis by applying a wavelet analysis (WA) method on the "a" wave of ERG signals obtained from individuals with congenital stationary night blindness, achromatopsia and normal. The determination of typical time-frequency features of the wave have been realized by using Mexican hat wavelet. It has been revealed out that the status of the retinal photoreceptors depends both the number of stable frequencies and their times of occurrences. In addition, when the pathological conditions have been taken into consideration, it has been found that the values of the frequency components have decreased and the formation times has changed [14]. In another study by Barraco et al., it has been analyzed the "a" wave of ERG signals recorded from normal subjects without eye disease at different flash intensities by the help of continuous wavelet transform (CWT). They have indicated that wavelet analysis applied by using Mexican hat is a quite effective signal processing method to determine the stable

---

frequencies and their times of occurrences of the ERG signals [15]. In 2014, it has been investigated which method is more successful by applying different signal processing methods on the "a" wave of ERG signals taken from congenital stationary night blindness, achromatopsia and normal subjects. In this respect, Fourier analysis (FA), principal component analysis (PCA) and WA have been used to distinguish healthy and pathological subjects. Thus, it has been found that WA using Mexican hat is a very successful method compared to PCA and FA methods [16]. In another study conducted in 2014, Gauvin et al. have utilized FA, CWT and discrete wavelet transform (DWT) methods to make time domain analysis of the photopic ERG signals of normal subjects. The performances of the methods has been compared with each other by detecting the peak amplitudes and times of the ERG signals. It has been shown that CWT applied by using Haar wavelet is the most proper method as compared to others [7].It has been analyzed the photopic ERG responses of the normal (healthy) subjects by using different signal processing techniques (short time Fourier transform (STFT), CWT and DWT) by Alaql. As a result of analysis, it has been found that CWT done with Daubechies (db) mother wavelet gives better results in time-frequency domain than the other methods [12].

On the other hand; obesity, which is one of the biggest health problems of today's world, has been growing rapidly in every day. It is a chronic disease which results from depending on the significant increase in body fat mass. The body mass index (BMI), calculated by dividing the body weight by the square of the height, is used by the World Health Organization (WHO) to evaluate the obesity level. According to this, it has been accepted that subjects with a BMI between 18 and 25 is normal, while between 25 and 30 are overweight, between 30 and 40 are obese, between 40 and 50 are morbid obese and over 50 are super obese [17]. Obesity is known to be associated with hypertension, type 2 diabetes, sleep apnea, coronary heart disease, stroke, dyslipidemia, gallbladder diseases, osteoarthritis, and even cancer. In addition, it has been reported that obesity effects visual acuity in negative manner and also causes many different eye diseases, such as cataract, age-related maculopathy, diabetic retinopathy and glaucoma [18–20]. However, to the best of our knowledge, there is no study that investigates the effects of obesity on ERG signals. In this context, the goal of this study is exhibited how the different classes of obesity affect the amplitudes and respective peak times of "a" and "b" waves of the ERG signals. To do this, we firstly identified and compared the amplitudes and peak times of the waves for normal and obese (obese, morbid obese, super obese) subjects based on statistical analysis. Then, the characteristic features of the waves for all group of subjects were investigated by applying STFT, CWT and DWT in time-frequency domain.

2. Material and methods

2.1. ERG dataset

In this study, ERG data of 40 people aged between 18 and 70 who applied to Zonguldak Bulent Ecevit University Obesity and Diabetes Application and Research Center were used. This data set consisting of normal, obese, morbid obese and super obese individuals shows a homogeneous distribution. Namely, each group contains data of 10 people.

The essential explanations have been given to all individuals before the test and all stages of the test have been carried out in accordance with the Zonguldak Bulent Ecevit University Human Research Ethics Committee and ISCEV (International Society for Clinical Electrophysiology of Vision) standards. In addition, an ophthalmological examination of each person have been performed by a specialist physician.

ERG signals have been taken by using Metrovision MonPackOne Electrooculography device provided within the scope of Zonguldak Bulent Ecevit University Scientific Research Project. Accordingly, Dawson-Trick-Litzkow (DTL) plus electrodes have been placed in the lower conjunctival sac of both eyes dilated priory. The ground and reference electrodes have been positioned in the center and sides of the
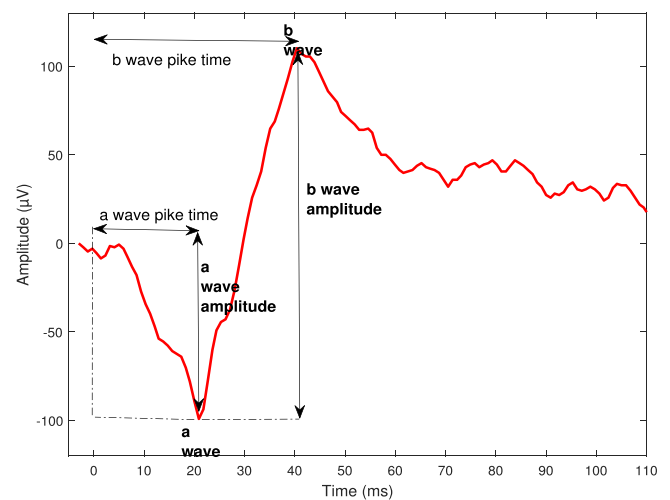
Fig. 1. The sample of ERG signal taken from a normal subject in time domain.

forehead, respectively. Then, the electrical responses of both of the eyes to the flash stimulus at different light intensity sent from the device have been recorded after a dark adaptation period of 20 min. Similar steps of the test have also been performed after a 15 min light adaptation period.

2.2. Basic features of ERG signals

ERG signals have two main components whose named as "a" and "b" waves as shown in Fig. 1. The first negative wave of the signal is called as "a" wave, which stems from the responses of photoreceptor cells (cones and rods). Its amplitude is measured from the pre-stimulus baseline to the most negative trough of the "a" wave, whereas its peak time is identified as the time elapsed from the flash onset to the "a" wave's peak. The "b" wave related to the bipolar cells is the highest positive wave following the "a" wave. The amplitude and peak time of the "b" wave, respectively, are determined from the peak-to-peak amplitude from the peak of the "b" wave to the trough of the "a" wave and from the flash onset to the peak of the "b" wave. The amplitudes and respective peak times of these waves, which can be measured by separating from cones and rod responses, can change by depending on the nature of the disease [7–12]. Thus, these measurements are great of importance for the interpretation of ERG signals.

For interpretation ERG signals, it is commonly utilized five ERG responses that are put forward by ISCEV. These are rod response, cone response, maximal response, 30 Hz flicker response and oscillatory potentials. In this study, the first three responses were taken into consideration in the analyses. Among them, rod response is the first signal after dark adaption. Maximal combined response originates from the responses of both cone and rod cells after dark adaption. Cone response arises from cone responses after light adaption [21].

2.3. ERG signal processing

Bio-signals recorded from organs in human body can contain significant information which cannot be distinguished by naked eye. To elicit characteristic features of this information giving rise to them, many different analytical methods have been developed. Selection of the proper method helps to comprehend the underlying physiological processes and to reveal accurate medical diagnoses. In this context, principle component analysis (PCA), Fourier analysis (FA) and wavelet analysis (WA) are commonly used in ERG signal analyses. Among them, wavelet analysis which allows the signals to be analyzed in the time-frequency domain is proposed as the most proper method in the recent studies [7,12,14–16].

2.4. Time-frequency analysis

Biomedical signals are non-stationary waves obtained from electrical activities of the human organs and they also provide sufficient information. The time-frequency analysis has been used as a powerful tool in practice to extract significant information from non-stationary signals [22].

2.4.1. Short time Fourier transform

Non-stationary signals have statistic characteristics changing over time. The Fourier transform is not convenient to analyze of these signals and it does not give information about how that frequency changes over time [22,23]. Therefore, the short time Fourier transform has been developed. In the STFT method, non-stationary signals are transform a stationary signal by using a window function. Then the STFT of the signal is obtained by taking the Fourier transform (FD) of each decomposed signal. STFT is defined as follows:

$$\text{STFT}(t,f) = \int_{-\infty}^{\infty} x(\tau)w^*(\tau - t)e^{-j2\pi f\tau}d\tau, \tag{1}$$

where $x(t)$ is the signal, $w(t)$ is the window function, * represents complex conjugate, f is the frequency, t is the time of displacement and τ represents slides the window through the waveform.

2.4.2. Continuous wavelet transform

The first proposed method to analyze frequency components of the signals is Fourier transform. The spectrum analysis of signals is performed by using of this transform. The properties of the signal in time domain are lost, while its properties in frequency domain are obtained by Fourier transform. Time-frequency domain representation of a signal is performed by windowing technique in Short Time Fourier Transform. But, it cannot be possible to carry out the time-frequency domain analysis efficiently with this technique due to the constant window length [24,25]. Therefore, CWT method including variable windowing properties has been proposed. By using this method, it can be possible to obtain better frequency resolution for low frequency components and better time resolution for high frequency components [24,26,27]. Analysis of a time series by CWT necessitates a set of functions obtained from mother wavelet ($\psi(t)$). $\psi(t)$ is expressed as follows:

$$\psi_{s,\tau}(t) = \frac{1}{\sqrt{|s|}}\psi\left(\frac{t-\tau}{s}\right) \rightleftharpoons \sqrt{|s|}\Psi(s\omega)e^{-j\omega\tau}, \tag{2}$$

where "s" and "τ" are the scaling and translation parameters, respectively. $\frac{1}{\sqrt{|s|}}$ is the normalization factor that ensures the same energy for whole "s" and "τ" [28–30]. When a mother wavelet is given, CWT of a signal $x(t)$ is expressed by the convolution of $x(t)$ with the complex conjugate of $\psi_{s,\tau}(t)$, as is given by the following equation:

$$X_\psi(s,\tau) = \left\langle x(t), \psi_{s,\tau}(t) \right\rangle = \int_{-\infty}^{\infty} x(t)\psi_{s,\tau}^*(t)dt, \tag{3}$$

where * demonstrates the complex conjugate operation. This equation can be written in the Fourier domain, considering the Parseval's relation [30]:

$$X_\psi(s,\tau) = \frac{\sqrt{|s|}}{2\pi} \int_{-\infty}^{\infty} X(\omega)\Psi^*(s\omega)e^{j\omega\tau}d\omega, \tag{4}$$

In this equation, the main factor is mother wavelet type and there are many kinds such as Haar, db, Mexican Hat, Morlet, Coiflet, Symlet. The selected wavelet type exhibits variety depending the application area. If the wavelet type were selected properly, the similarity between the signal and the wavelet type would be better [31]. Thus, it is great of importance to determine the proper mother wavelet. To analyze ERG signals, diverse mother wavelets types have been used. To the best of our knowledge, in literature, it has not been come across any studies that

Table 1
Peak times and amplitudes in rod responses.

Obesity classes	Waves	Amplitude (μv)	Time (ms)
Normal	a	13.93 ∓ 11.81	23.84 ∓ 16.94
	b	116.19 ∓ 48.30	84.51 ∓ 21.36
Obese	a	9.38 ∓ 10.58	25.22 ∓ 15
	b	131.33 ∓ 104.40	87.04 ∓ 11.08
Morbid obese	a	10.10 ∓ 11.11	27.34 ∓ 16.01
	b	129.77 ∓ 35.94	84.67 ∓ 13.03
Super obese	a	9.5 ∓ 9.15	34.8 ∓ 6.63
	b	102.45 ∓ 32.55	79.99 ∓ 7.13

reveal which type of wavelet is most suitable for ERG signal processing of obese subjects. In this study, we have used different wavelets type (db10, Haar, Mexican hat) and determined the proper one for this aim.

2.4.3. Discrete wavelet transform

DWT is a time-frequency analysis method in which the signal is separated into detail and approach coefficients using low and high pass filters. As a result of the signal passing through the high-pass filter, the approach coefficients are obtained, and by passing the low-pass filter, the detail coefficients are received [32]. DWT is calculated as follows:

$$\psi_{j,k}(t) = 2^{-j/2}\psi\left(2^{-j}t - k\right) \tag{5}$$

where 'j' and 'k' are the scale and translation parameters, respectively [30,31]. The DWT can be defined as a filtering operation with two related FIR filters, low-pass filter ($\phi(t)$) and high-pass filter ($\psi(t)$). The low pass and high pass wavelet filter coefficients specify the form of the scaling function ($\phi(t)$) and wavelet function ($\psi(t)$). Subsampling the signal by two will ensure to be discarded every other sample. Thus, the scale of the signal, which is expressed mathematically as the dilation equation and wavelet equation, is doubled. The dilation equation and wavelet equation are given as follows;

$$\phi(t) = \sum_k c_k\phi(2t - k), \tag{6}$$

$$\psi(t) = \sum_k d_k\phi(2t - k), \tag{7}$$

where c_k and d_k are coefficients of the low pass and high pass filters, respectively [28,33]. In the method, many different wavelet types are used to obtain a good resolution and realistic measurement. In this study, db10 and Haar wavelet types were used to determine which is more proper in the analysis of ERG signal.

2.5. Statistical analyses

ERG parameters of normal and different obesity groups have been estimated by using variant analytical approach such as mean value and standard deviation. We have utilized Z-scores and set a level of relevance of %5 by using SPSS 22.0 (Statistical Package for the Social Sciences) packet program.

Table 2
Peak times and amplitudes in maximal combined responses.

Obesity classes	Waves	Amplitude (μv)	Time (ms)
Normal	a	16.03 ∓ 5.95	13.97 ∓ 1.59
	b	55.83 ∓ 13.39	27.98 ∓ 1.42
Obese	a	10.00 ∓ 14.85	15.05 ∓ 1.14
	b	52.47 ∓ 18.25	29.92 ∓ 1.76
Morbid obese	a	13.71 ∓ 3.72	15.57 ∓ 1.73
	b	65.71 ∓ 36.15	30.80 ∓ 2.91
Super obese	a	66.27 ∓ 46.43	16.90 ∓ 7.96
	b	213.43 ∓ 140.22	46.4 ∓ 33.99

Table 3
Peak times and amplitudes in cone responses.

Obesity classes	Waves	Amplitude (μv)	Time (ms)
Normal	a	80.76 ∓ 47.24	16.29 ∓ 8.67
	b	159.00 ∓ 87.88	33.64 ∓ 17.99
Obese	a	113.35 ∓ 34.76	20.91 ∓ 2.00
	b	226.30 ∓ 62.75	43.93 ∓ 5.45
Morbid obese	a	118.01 ∓ 39.50	21.27 ∓ 2.59
	b	243.70 ∓ 65.83	44.47 ∓ 3.10
Super obese	a	15.06 ∓ 4.16	14.73 ∓ 0.81
	b	56.38 ∓ 18.19	30.01 ∓ 1.11

3. Results

In this study, we analyzed ERG signals for normal and three obesity groups (obese, morbid obese and super obese) in time and time-frequency domains. In the analysis; "a" and "b" waves in rod, cone and maximal combined responses of all groups have taken into consideration by averaging of 10 subjects' signals. Firstly, we obtained time and amplitude measurements of "a" and "b" waves for all groups in time domain by using statistical analysis. The obtained statistical results are given in Tables 1–3.

As seen in Table 1, in rod responses, when the peak times of "a" and "b" waves of obese subjects are compared with those of normal subjects, peak times of obese subjects have shifted to the right side (about 2 ∓ 6 ms). Besides the amplitude of "a" wave of obese subjects decreases about %33, while the amplitude of "b" wave increases about %13. The amplitudes of "b" waves have decreased in conjunction with obesity level, for all obese groups, whereas the amplitudes of "a" waves have not changed significantly. In addition, the peak times of "a" and "b" waves for obese and morbid obese subjects have shifted to right (about 2 ∓ 1 ms) and left sides (about 2 ∓ 2 ms), respectively. The peak times of the waves for super obese subjects have moved to right side about 9 ∓ 8 ms and left side about 7 ∓ 4 ms as compared with those for obese

subjects.

In maximal combined responses; the peak times of "a" waves for all subjects are close to each other, while the peak times of "b" waves have been increased in conjunction with obesity level (Table 2). On the other hand, the amplitudes of the waves for obese subjects decreases about % 38 and %6 in comparison with normal subjects, respectively. The amplitudes of the waves have increased in conjunction with obesity level for all obese groups. The rates of increment have been observed highest for super obese subjects.

As shown in Table 3, when the obese subjects are compared with normal subjects, the peak times of "a" and "b" waves shift towards about 4 ∓ 5 and 10 ∓ 10 ms of right side, respectively. Also, the amplitudes of the waves rise about %41. For obese and morbid obese subjects, it has not been observed considerable change in both the peak times and amplitudes of the waves. But for super obese subjects, the amplitude of "a" wave decreases by 7 times and the amplitude of "b" wave decreases about 3 times with respect to obese subjects. Also, the peak times of the waves shift towards (about 6 ∓ 1 ms) and (about 14 ∓ 4 ms) left side, respectively.

Secondly, we analyzed ERG components (namely, "a" and "b" waves) involved in rod, cone and maximal combined responses by using STFT, CWT and DWT in time-frequency domain. In this regard, analyzes are primarily carried out with STFT for each subject groups. The obtained results are given in Figs. 2–5.

As seen in the Figs. 2–5; when the energy levels are analyzed for 3 different ERG responses obtained from normal, obese, morbid obese and super obese subjects, it is seen that the frequencies of "a" and "b' waves are not obtained separately since the energy range in the frequency domain is wide scale. Hence the individual locations of the waves cannot be determined. Then, we analyzed ERG components (namely, "a" and "b" waves) involved in rod, cone and maximal combined responses for normal by using CWT in time-frequency domain. In this context, db10, Haar, Mexican hat wavelet types, which are commonly applied for ERG signal processing in literature, have been used in the analysis. The
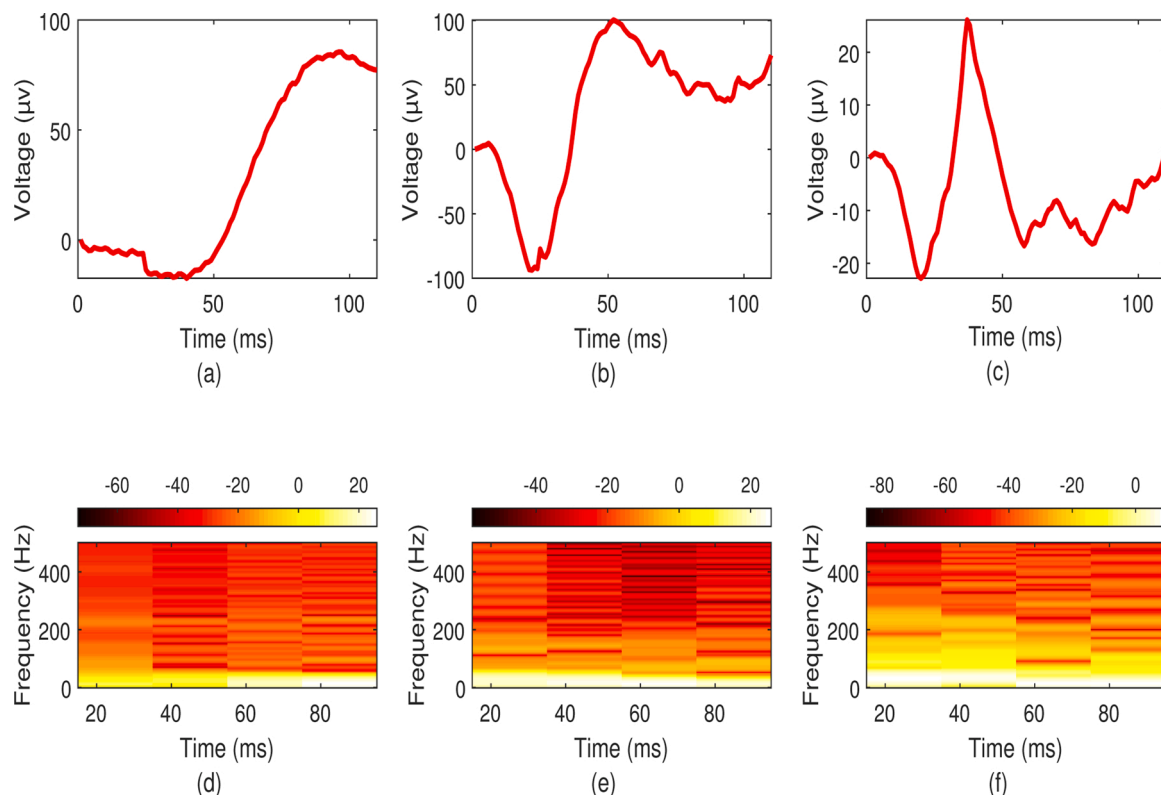
Fig. 2. Analysis of different responses of ERG signals obtained by the average of 10 normal subjects. The panel (a), (b) and (c) show rod, maximal combined and con responses, respectively. The panels (d), (e) and (f) represent STFT analysis of corresponding responses.
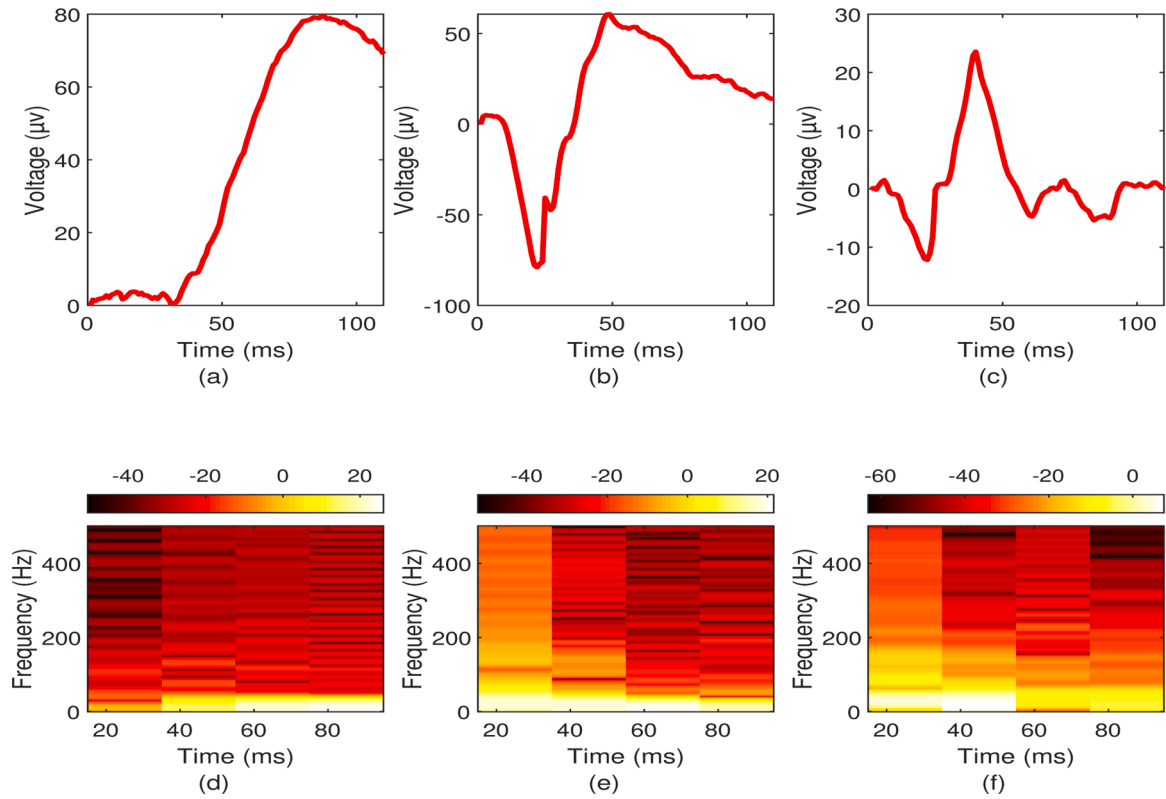
Fig. 3. Analysis of different responses of ERG signals obtained by the average of 10 obese subjects. The panel (a), (b) and (c) show rod, maximal combined and con responses, respectively. The panels (d), (e) and (f) represent STFT analysis of corresponding responses.
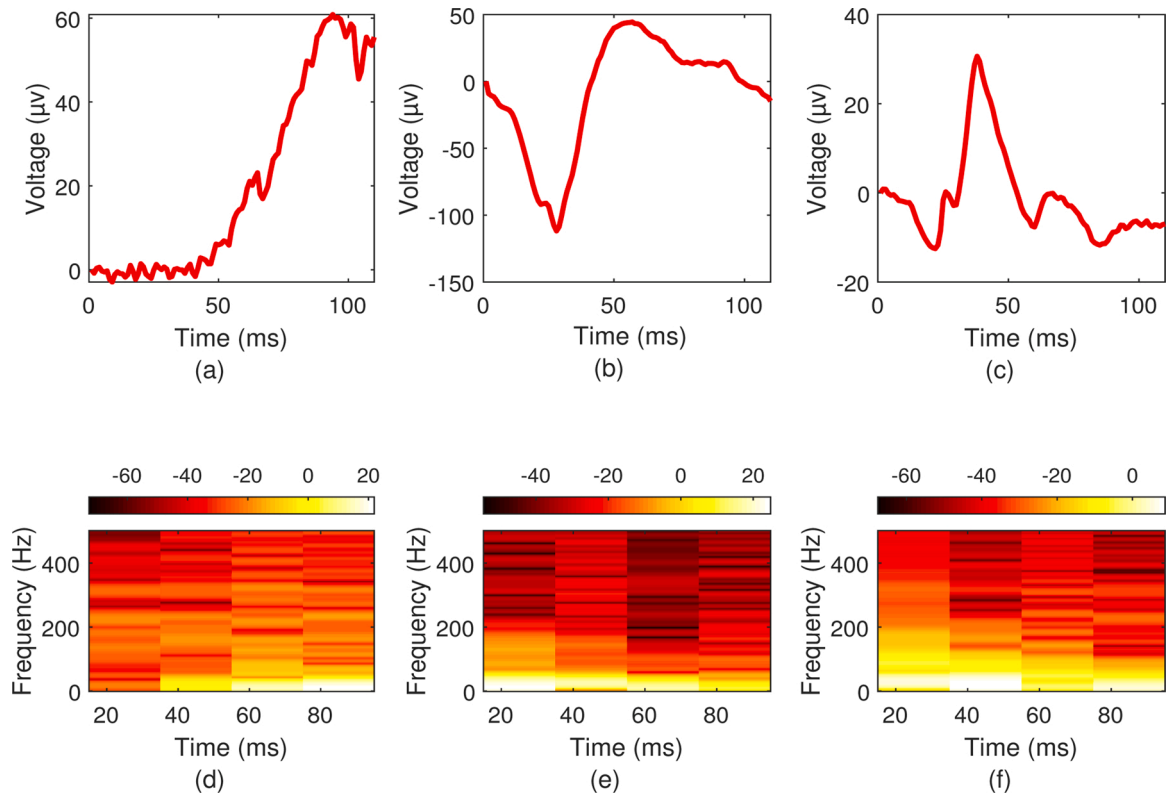
Fig. 4. Analysis of different responses of ERG signals obtained by the average of 10 morbid obese subjects. The panel (a), (b) and (c) show rod, maximal combined and con responses, respectively. The panels (d), (e) and (f) represent STFT analysis of corresponding responses.
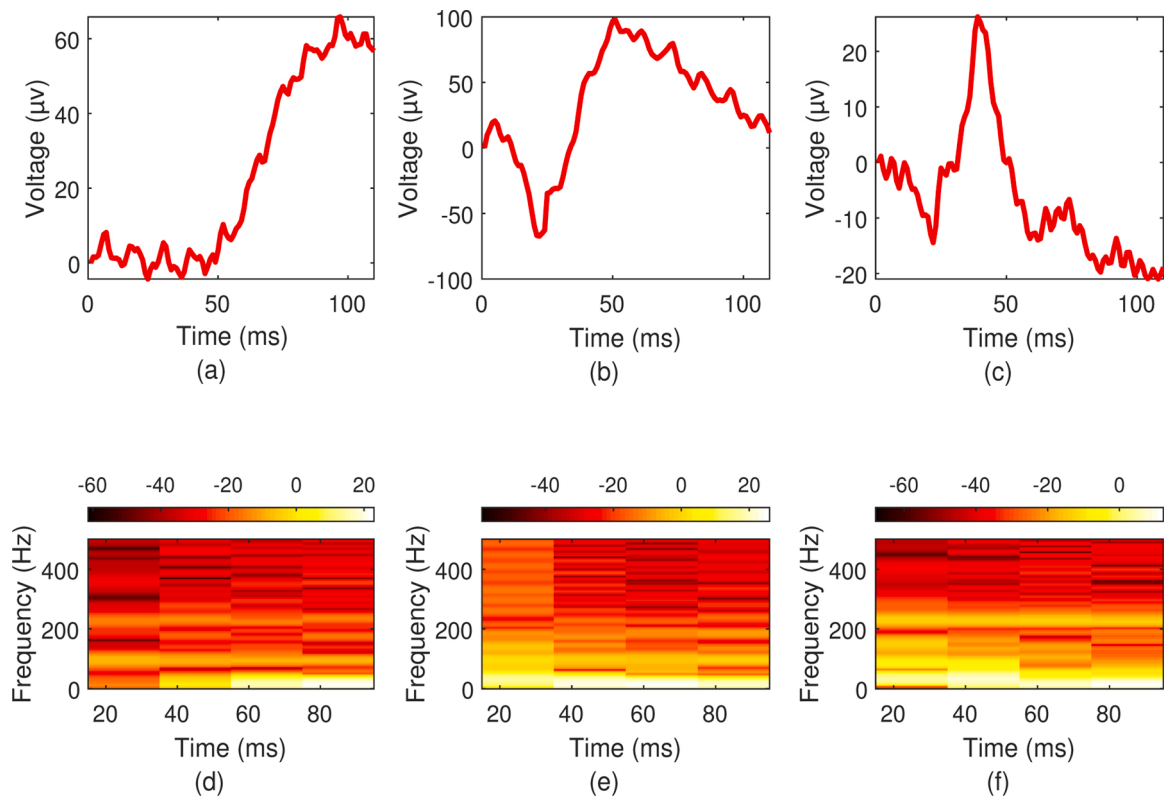
Fig. 5. Analysis of different responses of ERG signals obtained by the average of 10 super obese subjects. The panel (a), (b) and (c) show rod, maximal combined and con responses, respectively. The panels (d), (e) and (f) represent STFT analysis of corresponding responses.

energy levels of the waves have been extracted with usage of color scalogram to determine the best wavelet type. The obtained results are given in Fig. 6.

As seen in Fig. 7, when the energy levels were analyzed for 3 different responses of ERG signals (rod, cone and maximal combined responses), it has been seen that the Mexican wavelet is the most accurate wavelet type to determine the localization of "a" and "b" waves, while the other wavelets have caused in time shift. After determining the best wavelet type, finally, we have considered ERG components of the three responses for normal and obesity groups. Figs. 7–10 shows the obtained results.

The respective frequencies of "a" and "b" waves are extracted from the clustering regions in the color scalogram (Figs. 7–10). The figures also represent the energy levels of the ERG signals related with the amplitudes of the waves in 10–50 Hz frequency range against time. The intense energy levels in the color scalogram correspond to the localizations of "a" and "b" waves, respectively. The extractions of Figs. 7–10 are summarized in Table 4 for all responses of normal and obesity groups.

As seen in Table 4, in rod response, the "a" waves of ERG signals cannot be observed. In the maximal combined response; the peak time of the "a" wave for the normal subjects is 24 ∓ 4 ms, while those for the obesity groups (obese, morbid obese and super obese) are 23 ∓ 4, 25 ∓ 5 and 24 ∓ 3 ms. Besides, the frequencies have been obtained 41 ∓ 9, 40.5 ∓ 9, 38 ∓ 10 and 40 ∓ 10 Hz for normal and all obese subjects, respectively. Considering the cone response for all subject groups, in turn, it has been observed that the peak times are at 20 ∓ 2, 20 ∓ 1, 20 ∓ 2 and 20 ∓ 4 ms, whereas the frequencies are at 48.2 ∓ 2, 49.4 ∓ 1, 48.5 ∓ 2 and 45 ∓ 5 Hz.

On the other hand, the peak times of "b" waves at rod response have been sequentially obtained at 90 ∓ 6, 85 ∓ 7, 93 ∓ 5 and 92 ∓ 3 ms for normal and obesity groups. The frequencies have located at 23 ∓ 6 Hz for normal subjects, 21 ∓ 9 Hz for obese subjects, 28 ∓ 11 Hz for morbid

obese subjects and 25 ∓ 8 Hz for super obese subjects. In the maximal combined response, the peak time of the "b" wave for normal subject is 52 ∓ 5 ms, the peak times for the obesity groups are 55 ∓ 4, 54 ∓ 4 and 60 ∓ 4 ms. The wave frequency of normal subject is at 37 ∓ 8 Hz, while those of obesity groups have detected at 32 ∓ 6, 38 ∓ 6 and 24 ∓ 5 Hz, respectively. When the cone responses are analyzed, it has been revealed that the peak time and frequency of the "b" wave found at 40 ∓ 2 ms and 47 ∓ 2 Hz. Considering the responses for obesity groups, the peak times and frequencies have been located at 41 ∓ 4 ms and 44 ∓ 6 Hz for obese subjects, 40 ∓ 2 ms and 46 ∓ 4 Hz for morbid obese subjects, 40.5 ∓ 2 ms and 45.5 ∓ 4 Hz for super obese subjects.

Finally, we analyzed rod, cone and maximum combined responses of normal subjects with DWT using db10 and Haar wavelet types which are the most suitable wavelet types specified in the literature for ERG signal analysis [7,12]. The best wavelet type was primarily determined with color scalogram for normal subjects. The obtained results are shown in Fig. 11.

As shown in Fig. 11, the waves "a" cannot be observed in rod response similar to CWT analysis for each wavelet types. If the db10 is selected as mother wavelet type in DWT, the location of the waves "a" and "b" in each response can be accurately determined for the maximal combined and con responses. On the other hand; when the Haar wavelet is selected, the location of the waves "b" can be observed for the rod response, the locations of the "a" and "b" waves can only be determined in the maximal combined response. Besides, in cone response, the locations of the waves cannot be observed because of revealing a collective information (Fig. 11.i). Consequently, the db10 is obtained as the best suitable wavelet type in the DWT analysis of ERG signals. In this context, we apply DWT analysis on ERG signals for all subject groups and show the obtained results in Figs. 12–15.

The respective frequencies extracted from the clustering regions in the color scalogram (Figs. 12–15) show that the energy levels of the ERG signals for all subject groups are observed in 20–140 Hz frequency range
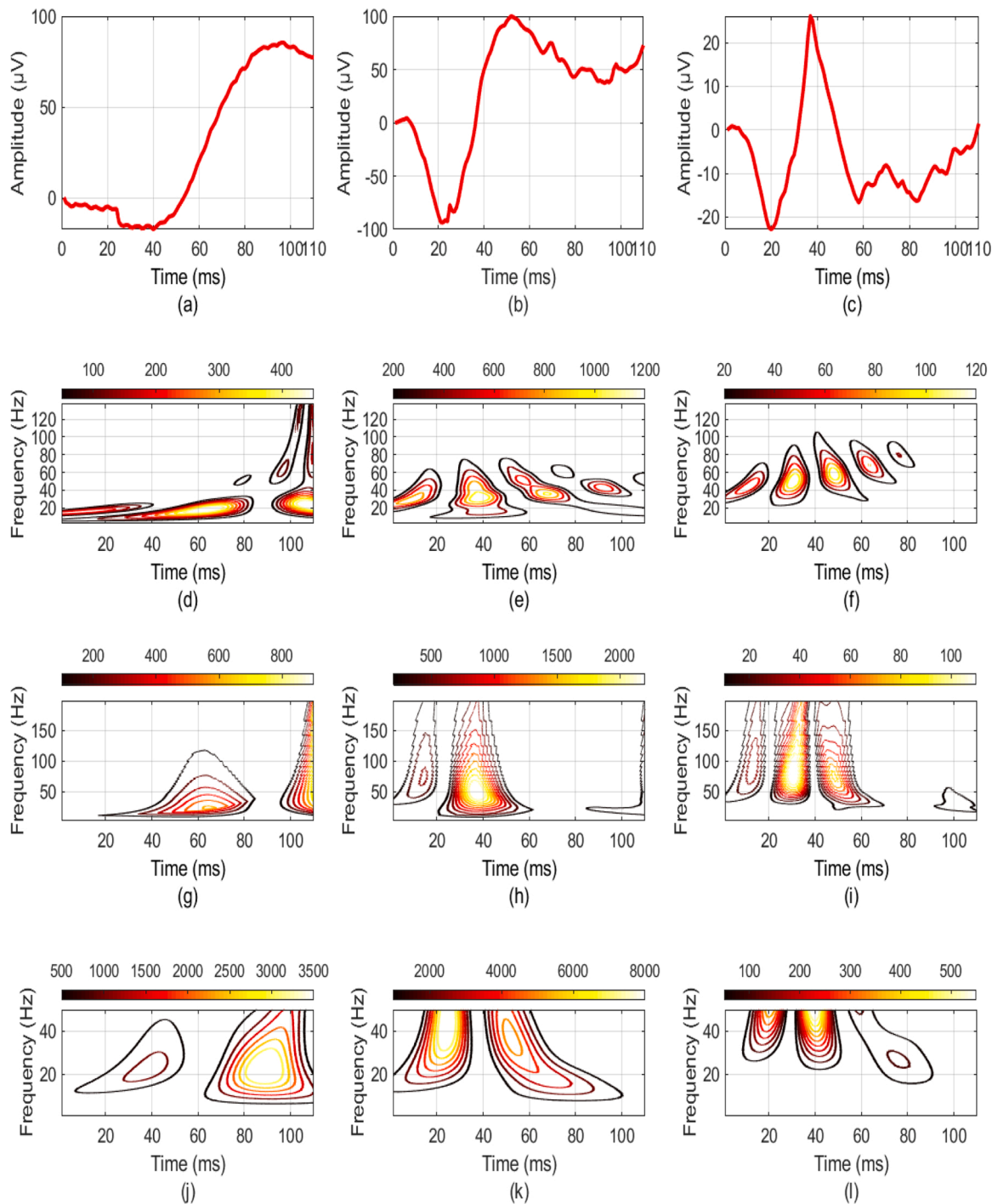
Fig. 6. Analysis of different responses of ERG signals obtained by the average of 10 normal subjects. The panel (a), (b) and (c) show rod, maximal combined and con responses, respectively. CWT analysis of different responses (rod, cone and maximal combined) of averaged ERG signals of normal subjects are given in the panel (d)–(l). The panel (d), (e) and (f) indicate the results of CWT analysis with db10 for three ERG response. The panel (g), (h) and (i) give the results of analysis with Haar wavelet. The panel (j), (k) and (l) show the results of analysis with Mexican hat wavelet.
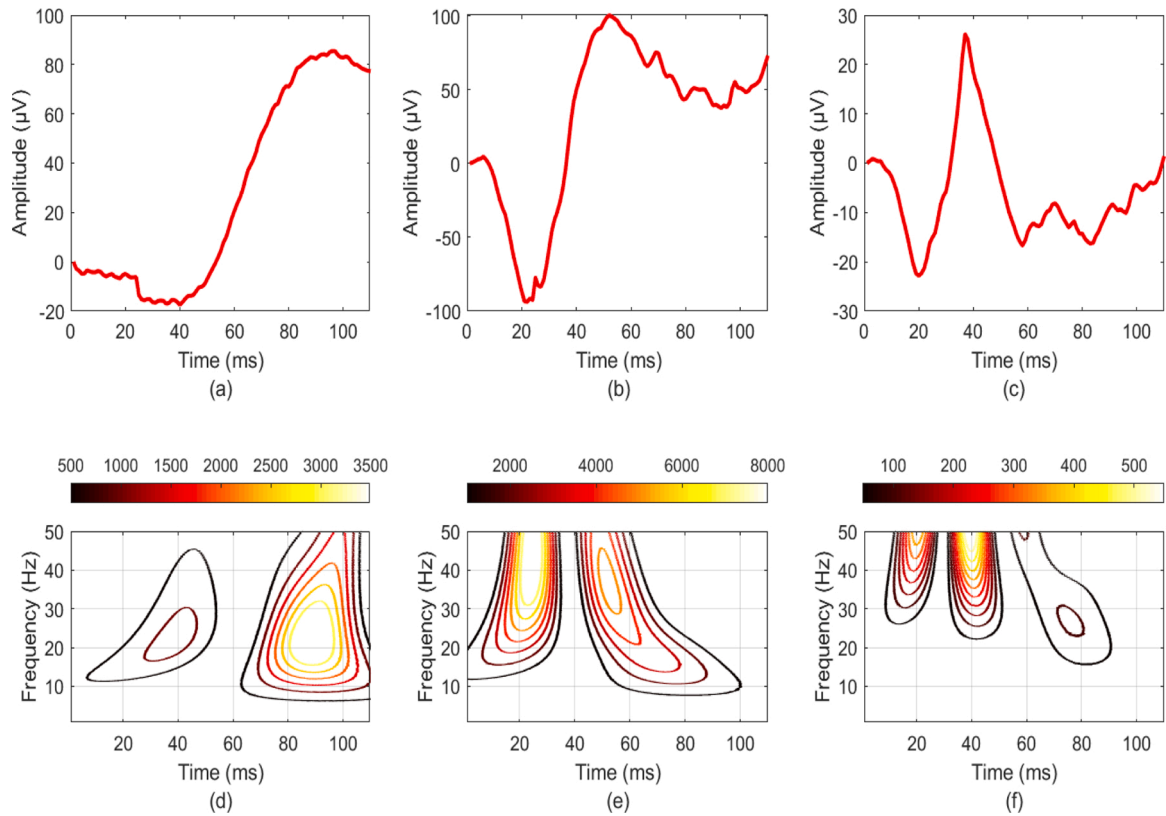
Fig. 7. Analysis of different responses of ERG signals obtained by the average of 10 normal subjects. The panel (a), (b) and (c) show rod, maximal combined and con responses, respectively. The panels (d), (e) and (f) represent CWT analysis with Mexican Hat wavelet of corresponding responses.
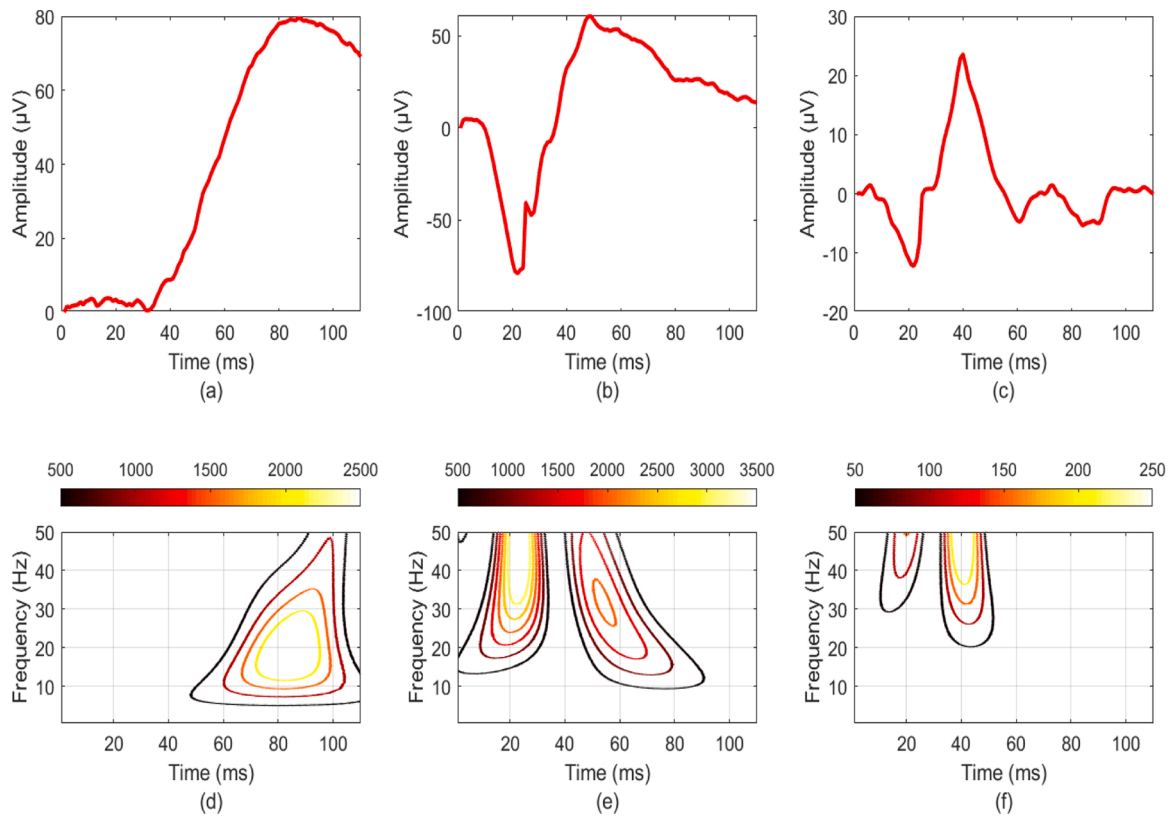
Fig. 8. Analysis of different responses of ERG signals obtained by the average of 10 obese subjects. The panel (a), (b) and (c) show rod, maximal combined and con responses, respectively. The panels (d), (e) and (f) represent CWT analysis with Mexican Hat wavelet of corresponding responses.
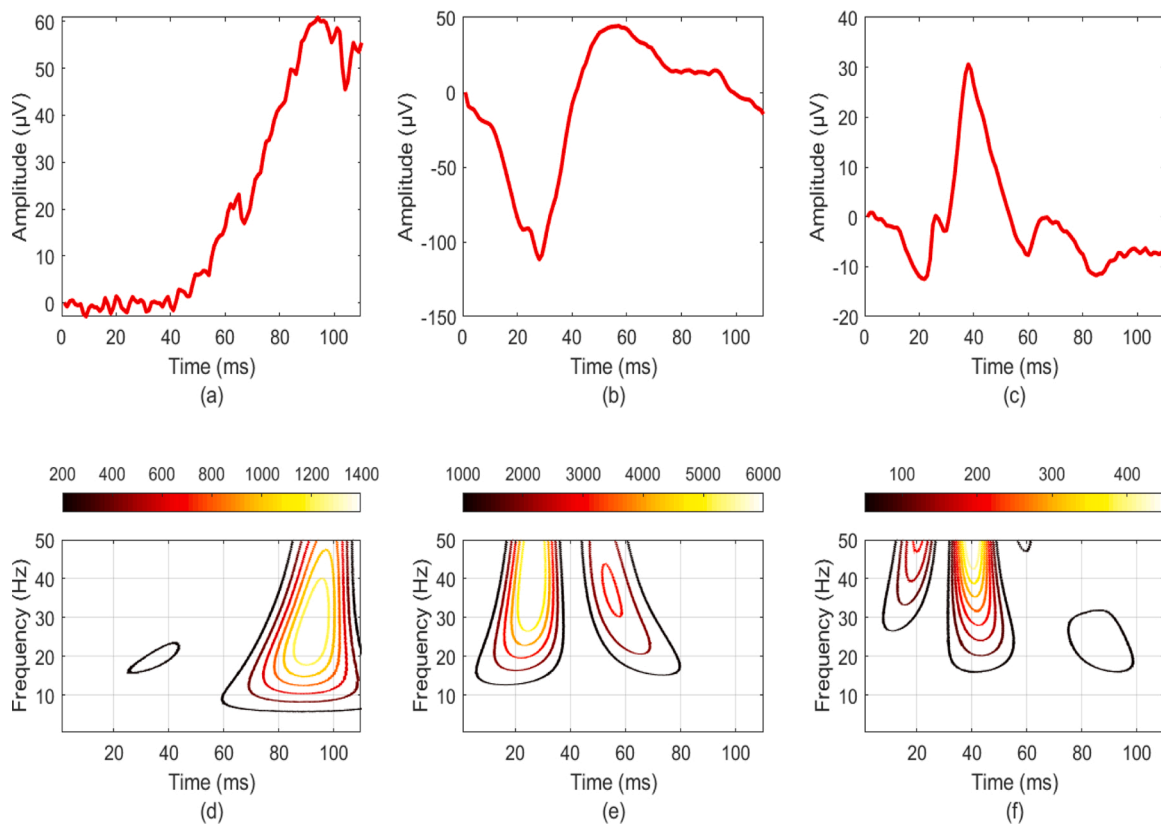
Fig. 9. Analysis of different responses of ERG signals obtained by the average of 10 morbid obese subjects. The panel (a), (b) and (c) show rod, maximal combined and con responses, respectively. The panels (d), (e) and (f) represent CWT analysis with Mexican Hat wavelet of corresponding responses.
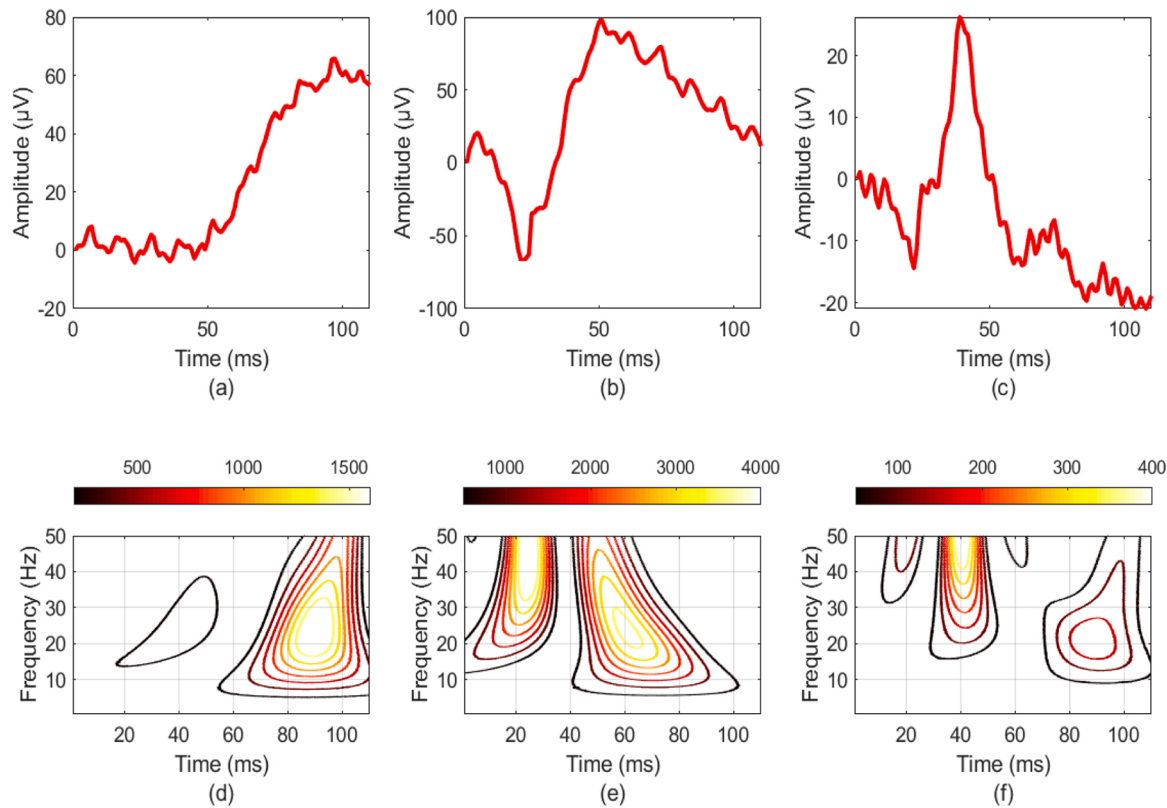
Fig. 10. Analysis of different responses of ERG signals obtained by the average of 10 super obese subjects. The panel (a), (b) and (c) show rod, maximal combined and con responses, respectively. The panels (d), (e) and (f) represent CWT analysis with Mexican Hat wavelet of corresponding responses.

Table 4
Values of the frequency components and times of occurrence extracted from rod, maximal combined and cone responses for normal and obesity groups using CWT.

	Rod response		Maximal combined response		Cone response	
	Time (ms)	Freq. (Hz)	Time (ms)	Freq. (Hz)	Time (ms)	Freq. (Hz)
Normal(a)	37∓9	23∓7	24∓4	41∓9	20∓2	48.2∓2
Normal(b)	90∓6	23∓6	52∓5	37∓8	40∓2	47∓2
Obese(a)			23∓4	40.5∓9	20∓1	49.4∓1
Obese(b)	85∓7	21∓9	55∓4	32∓6	41∓4	44∓6
Morbid Obese(a)			25∓5	38∓10	20∓2	48.5∓2
Morbid Obese(b)	93∓5	28∓11	54∓4	38∓6	40∓2	46∓4
Super obese(a)			24∓3	40∓10	20∓4	45∓5
Super obese(b)	92∓3	26∓8	60∓5	24∓5	40.5∓2	45.5∓4

against time. We extract time-frequency information with the intense energy levels in the color scalogram and have summarized in Table 5 for all responses of normal and obesity groups.

As shown in Table 5, the "a" wave is not observed in the rod response obtained from the ERG signal for all groups. In the maximal combined response; while the peak times of the "a" wave for the obesity groups (obese, morbid obese and super obese) are 25∓4, 27∓5 and 25∓2 ms, respectively, it is 25∓3 ms for the normal subjects. Besides, the frequencies have been obtained 132∓6, 129∓9, 125∓12 and 125∓11 Hz for normal and all obese subjects, respectively. In the cone response; while the peak time of the "a" wave cannot observed in obese and morbid obese subjects, for normal and super obese subject groups, the peak time of the "a" wave is obtained as 43∓2 and 42∓2 ms, respectively. The related frequencies of their have been obtained 133∓4 and 130∓7 Hz.

On the other hand, the peak times of "b" waves at rod response have been sequentially obtained at 96∓15, 89∓12, 96∓6 and 97∓13 ms for normal and all obesity groups. The frequencies have located at 137∓18 Hz for normal subjects, 132∓6 Hz for obese subjects, 132∓4 Hz for morbid obese subjects and 131∓5 Hz for super obese subjects. In the maximal combined response, the peak time of the "b" wave for normal subject is 51∓11 ms, the peak times of the "b" wave for all obesity groups are sequentially calculated as 50∓5, 54∓6 and 52∓6. While the "b" wave frequency of normal subject is at 128∓10 Hz, those of all obesity groups have obtained at 127∓10, 131∓6 and 130∓6 Hz, respectively. When the cone responses are analyzed, it has been revealed that the peak time and frequency of the "b" wave found at 63∓3 ms and 132∓6 Hz for normal subject. Considering the responses for all obesity groups, the peak times and frequencies have been located at 44∓3 ms and 13∓3 Hz, for obese subjects, 43∓4 ms and 126∓14 Hz for morbid obese subjects, 64∓2 ms and 133∓3 Hz for super obese subjects.

4. Discussion

The present paper is the first attempt to address the effects of obesity on ERG signals. On this aim, the rod, cone and maximum combined responses are obtained from ERG signals for each normal, obese, morbid obese and super obese subjects. Then these responses have been analyzed both in time and time-frequency domains to show effect of the obesity on ERG. We realize traditional statistical analysis to extract time domain components of signals. However, the traditional analysis methods may not give enough information about biomedical signal

dynamics. Therefore, the wavelet transform is widely used for signal analysis in time-frequency domains. In this context, we use time-frequency analysis methods analysis to obtain detailed signal components. These analyses help medical doctors to make ophthalmologic diagnosis in cases where they cannot be distinguished with the naked eye.

The analysis of the ERG signals are commonly performed by using its two major components named as the "a" and "b" waves, and hence we have used these waves in this study. In this context, firstly, we obtain the amplitudes and respective peak times of the "a" and "b" waves by using the statistical analysis based time domain on the rod, cone and maximum responses of the ERG signals in four different groups. The obtained results have shown that there are no significant differences among groups (Tables 1–3). Therefore, we apply three different time-frequency methods (STFT, CWT and DWT) on ERG signals; we have applied STFT analysis for all subject groups and it is founded that although the "a" and "b" waves are obtained from amplitude in the time domain, they cannot be observed since the energy range in the frequency domain is wide scale. Then we have applied CWT analysis using three different mother wavelets (db10, Haar, Mexican hat) on these responses and have found that the Mexican hat is the most proper mother wavelet type to determine the localizations of "a" and "b" waves. Meanwhile, we have extracted the time and frequency information of waves from the CWT analysis performed based on the Mexican hat wavelet. Finally, we have applied DWT analysis using different mother wavelets (db10, Haar) on these responses. It is found that the db10 is the most proper mother wavelet type to determine the localizations of "a" and "b" waves. When the results of the DWT analysis are compared with the CWT analysis, the "a" wave cannot be observed as in CWT analysis for the rod responses of obese subject groups in time and frequency domains, time-frequency information of "a" wave in the cone response of obese and morbid obese subjects could not be observed in DWT analysis, the "a" and "b" wave has not shown a considerable change for all ERG responses in DWT. On the other hand, for maximal combined response in CWT, the frequencies of the "b" wave of super obese subjects reduce significantly and also peak times shift towards to the right side at time as compared with normal subjects. In sum, it is proved that the CWT method based on the Mexican hat wavelet is proper to research obesity effects on ERG signals.

The main advantage of this study is that it reveals out that obesity known to have negative effects on human health also affects the retinal layer of the eye and another advantage of this study is that it reveals the effect of different obesity levels on the ERG signal. On the other hand, the potential limitation of this study is the dataset was composed of measurements taken from patients aged between 18 and 70 years. Therefore, the results of this study cannot be generalized to people under 18 years old. Another limitation is that the periods of adaptation in the measurements are selected as 20 min for the dark adaptation and 15 min for the light adaptation with ISCEV's recommendations.

5. Conclusion and future work

In this study, the effect of obesity on ERG signal was analyzed by using different signal processing methods (STFT, CWT and DWT) and it is seen that the CWT exhibits a better performance than other methods with respect to time-frequency results. It is also showed that the usage of Mexican hat is the most proper wavelet type to analyze obesity effect for ERG. Moreover, we demonstrated that wave "a" does not have a significant effect with obesity on ERG signals. On the contrary, the obesity has significantly effect on the "b" wave for maximal combined response with respect to the other responses of ERG. In this context, it can be
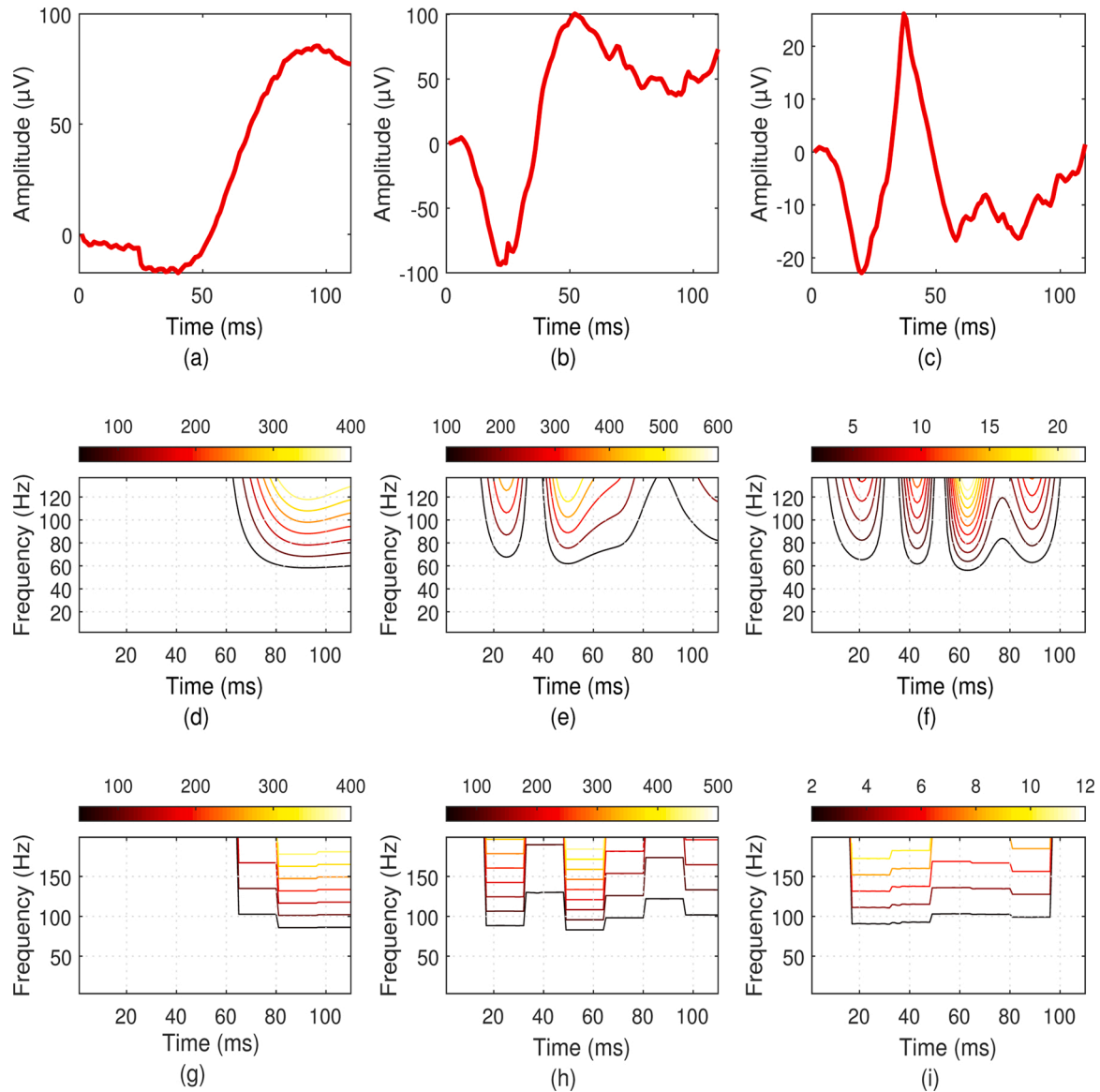
Fig. 11. Analysis of different responses of ERG signals obtained by the average of 10 normal subjects. The panel (a), (b) and (c) show rod, maximal combined and con responses, respectively. DWT analysis of different responses (rod, cone and maximal combined) of averaged ERG signals of normal subjects are given in the panel (d)–(i). The panel (d), (e) and (f) indicate the results of DWT analysis with db10 for three ERG response. The panel (g), (h) and (i) give the results of analysis with Haar wavelet.
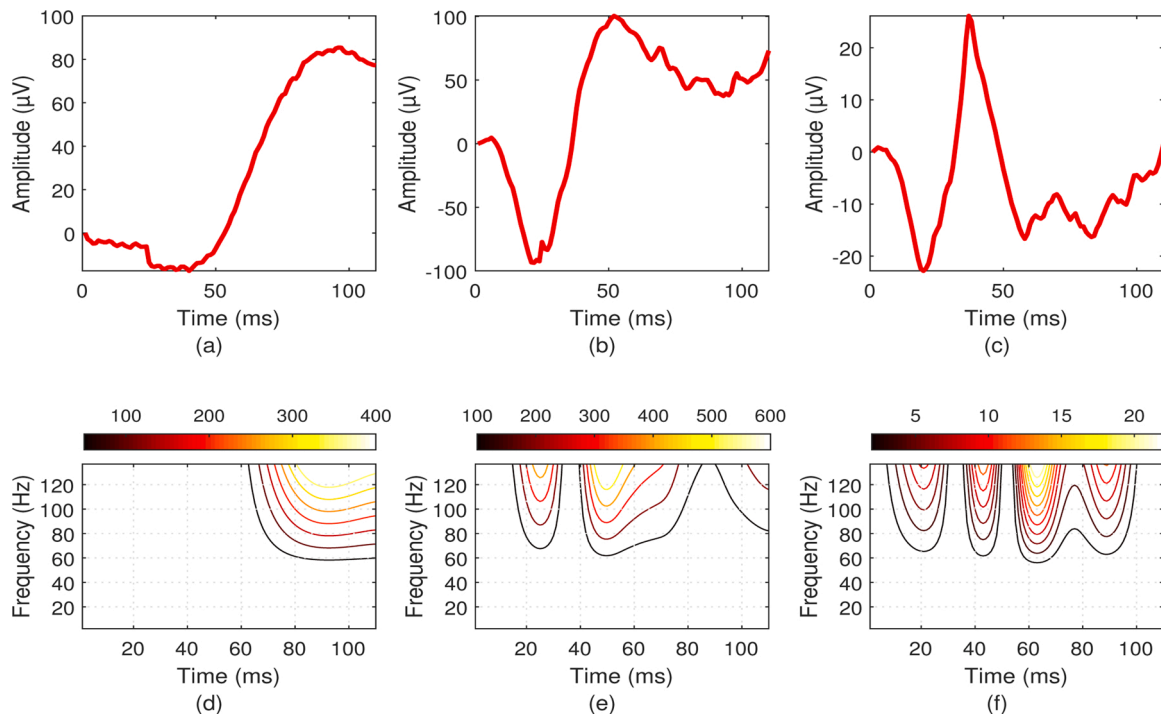
Fig. 12. Analysis of different responses of ERG signals obtained by the average of 10 normal subjects. The panel (a), (b) and (c) show rod, maximal combined and con responses, respectively. The panels (d), (e) and (f) represent DWT analysis with db10 wavelet of corresponding responses.
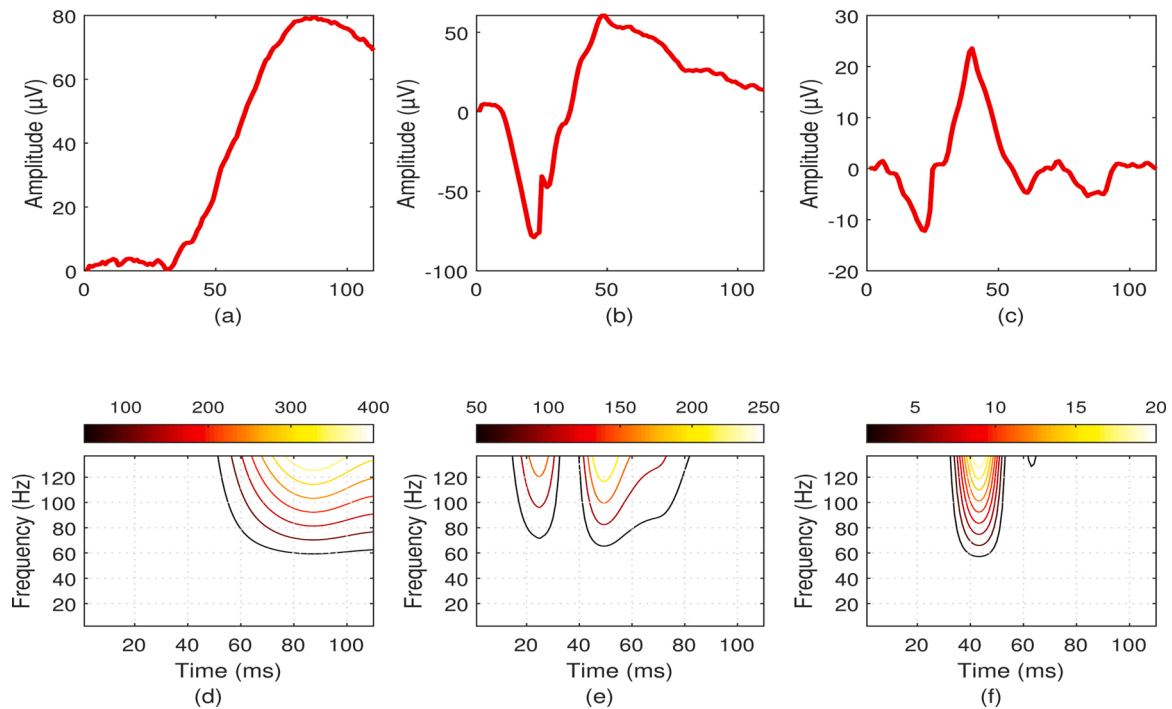
Fig. 13. Analysis of different responses of ERG signals obtained by the average of 10 obese subjects. The panel (a), (b) and (c) show rod, maximal combined and con responses, respectively. The panels (d), (e) and (f) represent DWT analysis with db10 wavelet of corresponding responses.

concluded that the levels of obesity adversely affect eye health.

The main limitations of this study are derived from the measurement process. In the future works, this issue will be addressed for the people under 18 years old and new datasets will be obtained. This process will be realized with different signal processing methods for all dataset. A decision support system based on classification will be designed with the obtained features. Traditional and novel classification (deep learning networks) methods will be used to classify obesity levels.

Authors' contribution

Conceptualization, methodology, validation, writing - original draft preparation and writing - review and editing: O.E., S.Y.I. and U.A.R.; supervision: O.E. and U.A.R.
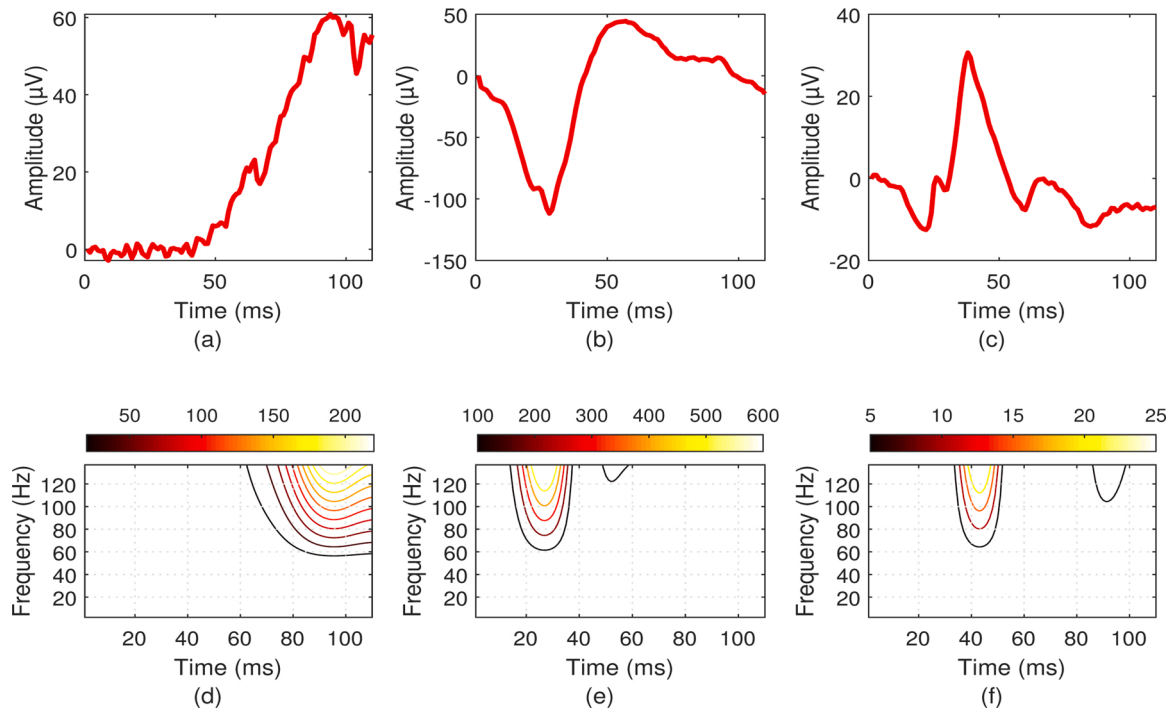
Fig. 14. Analysis of different responses of ERG signals obtained by the average of 10 morbid obese subjects. The panel (a), (b) and (c) show rod, maximal combined and con responses, respectively. The panels (d), (e) and (f) represent DWT analysis with db10 wavelet of corresponding responses.
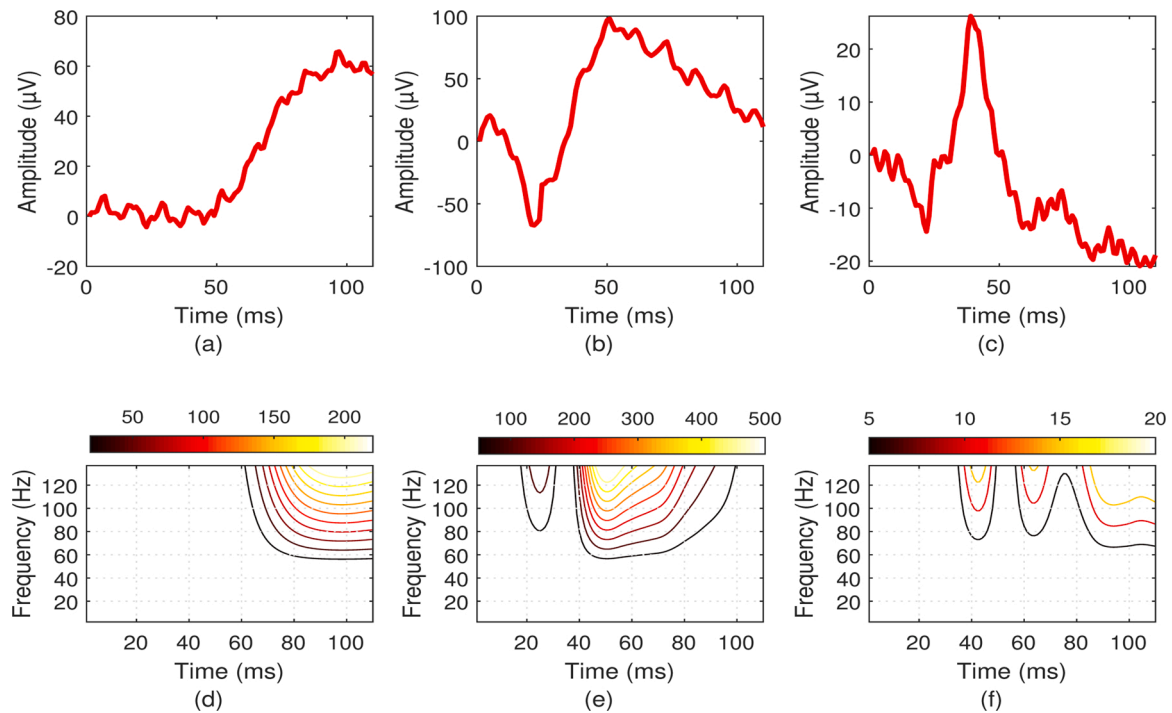
Fig. 15. DWT analysis of different responses of ERG signals obtained by the average of 10 super obese subjects. The panel (a), (b) and (c) show rod, maximal combined and con responses, respectively. The panels (d), (e) and (f) represent DWT analysis with db10 wavelet of corresponding responses.

Table 5

Values of the frequency components and times of occurrence extracted from rod, maximal combined and cone responses for normal and obesity groups obtained by DWT.

	Rod response		Maximal combined response		Cone response	
	Time (ms)	Freq. (Hz)	Time (ms)	Freq. (Hz)	Time (ms)	Freq. (Hz)
Normal(a)			25±3	132±6	43±2	133±4
Normal(b)	96±15	137±18	51±11	128±10	63±3	132±6
Obese(a)			25±4	129±9		
Obese(b)	89±12	132±6	50±5	127±10	44±3	133±3
Morbid obese(a)			27±5	125±12		
Morbid obese(b)	96±6	132±4	54±6	131±6	43±4	126±14
Super obese(a)			25±2	125±11	42±2	130±7
Super obese(b)	97±13	131±5	52±6	130±6	64±2	133±3

Acknowledgment

Declaration of Competing Interest

The authors report no declarations of interest.

References

[1] M. Marmor, G. Holder, M. Seeliger, S. Yamamoto, Standard for clinical electroretinography, Adv. Ophthalmol. 108 (2004) 107–114, https://doi.org/10.1023/B:DOOP.0000036793.44912.45.

[2] A. Fulton, R. Hansen, C. Westall, Development of erg responses: the iscev rod, maximal and cone responses in normal subjects, Adv. Ophthalmol. 107 (2003) 235–241, https://doi.org/10.1023/B:DOOP.0000005332.88367.b8.

[3] R. Granit, The components of the retinal action potential in mammals and their relation to the discharge in the optic nerve, J. Physiol. 77 (3) (1933) 207–239.

[4] T. Tomita, Studies on the intraretinal action potential part i. relation between the localization of micro-pipette in the retina and the shape of the intraretinal action potential, Jpn. J. Physiol. 1 (1950) 110–117, https://doi.org/10.2170/jjphysiol.1.110.

[5] G. Arden, A. Friedmann, H. Kolb, Anticipation of chloroquine retinopathy, Lancet 279 (7240) (1962) 1164–1165, https://doi.org/10.1016/S0140-6736(62)92200-6.

[6] J.A. Boughman, G.A. Fishman, A genetic analysis of retinitis pigmentosa, Br. J. Ophthalmol. 67 (7) (1983) 449–454, https://doi.org/10.1136/bjo.67.7.449.

[7] M. Gauvin, j.-m. Lina, P. Lachapelle, Advance in erg analysis: from peak time and amplitude to frequency, power, and energy, BioMed Res. Int. 2014 (2014) 246096, https://doi.org/10.1155/2014/246096.

[8] P.A. Sieving, K. Murayama, F. Naarendorp, Push-pull model of the primate photopic electroretinogram: A role for hyperpolarizing neurons in shaping the b-wave, Visual Neurosci. 11 (3) (1994) 519–532, https://doi.org/10.1017/S0952523800002431.

[9] D.C. Hood, D.G. Birch, Human cone receptor activity: the leading edge of the a-wave and models of receptor activity, Visual Neurosci. 10 (5) (1993) 857–871, https://doi.org/10.1017/S0952523800006076.

[10] R. Miller, J.E. Dowling, Intracellular responses of the müller (glial) cells of mudpuppy retina: their relation to b-wave of the electroretinogram, J. Neurophysiol. 33 (3) (1970) 323–341.

[11] R. Hamilton, M. Bees, C. Chaplin, D. McCulloch, The luminance-response function of the human photopic electroretinogram: a mathematical model, Vision Res. 47 (2007) 2968–2972, https://doi.org/10.1016/j.visres.2007.04.020.

[12] A.M. Alaql, Analysis and Processing of Human Electroretinogram, 2016.

[13] D.J. Creel, A.S. Crandall, F.A. Ziter, Identification of minimal expression of myotonic dystrophy using electroretinography, Electroencephalogr. Clin. Neurophysiol. (1985).

[14] R. Barraco, D. Persano Adorno, M. Brai, Wavelet Analysis of Human Photoreceptoral Response, 2010, pp. 1–4, https://doi.org/10.1109/ISABEL.2010.5702846.

[15] R. Barraco, D.P. Adorno, M. Brai, Erg signal analysis using wavelet transform, Theory Biosci. 130 (2011) 155–163.

[16] M. Brai, L. Tranchina, R. Barraco, D. Persano Adorno, A comparison among different techniques for human erg signals processing and classification, Default J. 30 (2014) 86–95.

[17] B. Dogan, C. Öner, Association of body fat ratio with anthropometric and lipid parameters measured by two different technique in obese persons, Demiroglu Science University Florence Nightingale J. Med. 1 (2015) 124, https://doi.org/10.5606/fng.btd.2015.023.

[18] N. Cheung, T.-Y. Wong, Obesity and eye diseases, Surv. Ophthalmol. 52 (2007) 180–195, https://doi.org/10.1016/j.survophthal.2006.12.003.

[19] N. Friedman, E. Fanning, Overweight and obesity: an overview of prevalence, clinical impact, and economic impact, Dis. Manag. 7 (Suppl. 1) (2004) S1–6, https://doi.org/10.1089/1093507042317152.

[20] D.W. Haslam, W.P.T. James, Obesity, Lancet 366 (9492) (2005) 1197–1209, https://doi.org/10.1016/S0140-6736(05)67483-1.

[21] S. Nair, P. Joseph, Chaotic analysis of the electroretinographic signal for diagnosis, BioMed Res. Int. 2014 (2014) 503920, https://doi.org/10.1155/2014/503920.

[22] Y. Yang, Z. Peng, W. Zhang, G. Meng, Parameterised time-frequency analysis methods and their engineering applications: a review of recent advances, Mech. Syst. Signal Process. 119 (2019) 182–221.

[23] R.M. Rangayyan, Biomedical Signal Analysis, vol. 33, John Wiley & Sons, 2015.

[24] B.K. Karaca, B. Oltu, T. Kantar, E. Kiliç, M.F. Aksahin, A. Erdamar, Classification of heart sound recordings with continuous wavelet transform based algorithm, 2018 26th Signal Processing and Communications Applications Conference (SIU) (2018) 1–4, https://doi.org/10.1109/SIU.2018.8404450.

[25] D.T. Nguyen, Y.H. Park, K.Y. Shin, S.Y. Kwon, H.C. Lee, K.R. Park, Fake finger-vein image detection based on Fourier and wavelet transforms, Digital Signal Process. 23 (5) (2013) 1401–1413, https://doi.org/10.1016/j.dsp.2013.04.001.

[26] L. Tawade, Detection of epilepsy disorder using discrete wavelet transforms using matlabs, Int. J. Adv. Sci. Technol. 28 (2011) 17–24.

[27] Y. Cengiz, Y.D.U. Ariöz, An application for speech denoising using discrete wavelet transform, 2016 20th National Biomedical Engineering Meeting (BIYOMUT) (2016) 1–4, https://doi.org/10.1109/BIYOMUT.2016.7849377.

[28] S.S. Nair, K.P. Joseph, Wavelet based electroretinographic signal analysis for diagnosis, Biomed. Signal Process. Control 9 (2014) 37–44.

[29] S. Mallat, A Wavelet Tour of Signal Processing, Elsevier, 1999.

[30] P. Singh, Novel generalized fourier representations and phase transforms, Digital Signal Process. 106 (2020) 102830.

[31] H. Eristi, A. Uçar, Y. Demir, Wavelet-based feature extraction and selection for classification of power system disturbances using support vector machines, Electr. Power Syst. Res. 80 (7) (2010) 743–752, https://doi.org/10.1016/j.epsr.2009.09.021.

[32] S.G. Mallat, A Theory for Multiresolution Signal Decomposition: The Wavelet Representation, 1989.

[33] J.N. Weiss, Treatment of central retinal vein occlusion by injection of tissue plasminogen activator into a retinal vein, Am. J. Ophthalmol. 126 (1) (1998).